chemosensors

*Article*

# Detection of Ammonia Nitrogen in Neutral Aqueous Solutions Based on In Situ Modulation Using Ultramicro Interdigitated Array Electrode Chip

**Yuqi Liu [1,2], Nan Qiu [1,2], Zhihao Zhang [1,2], Yang Li [1] and Chao Bian [1,*]**

[1] State Key Laboratory of Transducer Technology, Aerospace Information Research Institute, Chinese Academy of Sciences, Beijing 100190, China; liuyuqi222@mails.ucas.ac.cn (Y.L.); qiunan23@mails.ucas.ac.cn (N.Q.); zhangzhihao221@mails.ucas.ac.cn (Z.Z.); yangli@mail.ie.ac.cn (Y.L.)
[2] School of Electronic, Electrical and Communication Engineering, University of Chinese Academy of Sciences, Beijing 100049, China
* Correspondence: cbian@mail.ie.ac.cn

**Abstract:** In this study, an in situ electrochemical modulation method based on an ultramicro interdigitated array electrode (UIAE) sensor chip was developed for the detection of ammonia nitrogen ($NH_3$-N) in neutral aqueous solutions. One comb of the UIAE was used as the working electrode for both the modulating and sensing functions, while the other comb was used as the counter electrode. Utilizing its enhanced mass transfer and proximity effects, the feasibility of in situ modulation of the solution environment near the UIAE chip to generate an electrochemical response for $NH_3$-N was investigated using electrochemical methods. The proposed method enhances the concentration of hydroxide ions and active chloride in the local solution near the sensor chip. These reactive species play a key role in improving the sensor's electrocatalytic oxidation capability toward ammonia nitrogen, facilitating the sensitive detection of ammonia nitrogen in neutral environments. A linear relationship was displayed, ranging from 0.15–2.0 mg/L (as nitrogen) with a sensitivity of 3.7936 $\mu A \cdot L \cdot mg^{-1}$ (0.0664 $\mu A\ \mu M^{-1}\ mm^{-2}$), which was 2.45 times that in strong alkaline conditions without modulation. Additionally, the relative standard deviation of the measurement remained below 2.9% over five days of repeated experiments, indicating excellent stability.

**Keywords:** electrochemical sensing; ammonia nitrogen; micro-sensing electrode chip; ultramicro interdigitated array electrode chip; in situ electrochemical modulation

check for updates

Received: 8 March 2025
Revised: 3 April 2025
Accepted: 8 April 2025
Published: 9 April 2025

**Citation:** Liu, Y.; Qiu, N.; Zhang, Z.; Li, Y.; Bian, C. Detection of Ammonia Nitrogen in Neutral Aqueous Solutions Based on In Situ Modulation Using Ultramicro Interdigitated Array Electrode Chip. *Chemosensors* **2025**, *13*, 138. https://doi.org/10.3390/chemosensors13040138

**Copyright:** © 2025 by the authors. Licensee MDPI, Basel, Switzerland. This article is an open access article distributed under the terms and conditions of the Creative Commons Attribution (CC BY) license (https://creativecommons.org/licenses/by/4.0/).

## 1. Introduction

Ammonia nitrogen ($NH_3$-N) is a significant indicator of water quality. According to China's Environmental Quality Standards for Surface Water (GB 3838-2002), the permissible concentration range of $NH_3$-N in Class I to Class V surface water is 0.15–2.0 mg/L (as nitrogen). And, according to China's Standards for Drinking Water Quality (GB 5749-2022), the maximum permissible concentration of $NH_3$-N (as N) in drinking water is 0.5 mg/L. To meet these standards, rapid and sensitive detection of $NH_3$-N concentrations is essential for effective water resource management, enabling real-time monitoring and pollution control. It is essential to transition from conventional, laboratory-based water quality sampling and analysis to on-site, rapid detection of contamination while miniaturizing detection systems and improving their portability. At present, the electrochemical sensing technique is the primary approach for achieving on-site, rapid detection.

The term $NH_3$-N includes the non-ionized ammonia ($NH_3$) and ionized ammonium ($NH_4^+$) species. $NH_3$ and $NH_4^+$ can reach a dynamic dissociation equilibrium in water. The higher the pH or temperature of the water, the greater the molar percentage of $NH_3$ in the total $NH_3$-N content [1]. $NH_3$ has higher chemical reactivity. By applying an appropriate voltage, $NH_3$ can be catalytically oxidized on the surface of the electrode, usually a platinum electrode. During this process, $NH_3$ gradually dehydrogenates, facilitating charge transfer and generating an electrochemical response current [2–4]. Electrochemical sensors for $NH_3$-N detection based on this mechanism offer high specificity and strong anti-interference capabilities, and they have been widely used. Conventional electrodes, such as commercial disk electrodes, exhibit an inherently low sensitivity. Numerous studies have reported the use of nanocomposite-modified electrodes to enhance the sensitivity of $NH_3$-N detection in water. For instance, Qin et al. [5] modified carbon cloth electrodes with gold nanoparticles (AuNPs), Zhou et al. [6] with nickel-copper carbonate hydroxide, and Wang et al. [7] with platinum-zinc alloy nanoflowers. These modified electrodes achieved high detection sensitivity under laboratory conditions, along with reliable performance in real-water sample testing. However, due to the strong alkaline environments required for $NH_3$-N detection, corrosion resistance is a significant problem for both the sensing electrodes and the entire detection system.

From the perspective of micro-electromechanical systems (MEMS) integration, optimized sensing structures can enhance detection performance. Ultramicro interdigitated array electrodes (UIAEs), with their unique generation–collection effect at characteristic dimensions, significantly improve mass transfer efficiency between electrodes, leading to a notable increase in the response current density during electrocatalytic oxidation reactions [8–13]. Additionally, some studies have demonstrated that UIAEs can regulate the pH of the solution near the electrode surface by applying a certain potential or current [14–18]. In these methods, one comb of the UIAE is designated as the protonator electrode, while the other is designated as the sensor electrode. It is also necessary to incorporate a counter electrode and a reference electrode, as normally required in electrochemical experiments. These electrodes form a four-electrode system, and a double-channel electrochemical workstation is generally utilized for the experiments. Sullivan et al. [16] simulated the pH modulation effects of interdigitated electrodes under different potentials. When an appropriate potential or current is applied to the protonator electrode, protons are generated, leading to changes in the pH near the sensor electrode due to the influence of adjacent regions. Using this in situ modulation method, a neutral solution can be locally adjusted to an acidic condition (pH = 3), generating substances that promote redox reactions as catalysts. This allows the sensor electrode to perform target detection without the need for additional strong acids. Based on this principle, Seymour et al. [15] achieved the detection of free chlorine, and Wasiewska et al. [18] detected silver ions. These results provide effective pathways for interdigitated electrodes to achieve electrochemical responses in near-neutral environments rather than in extreme pH conditions.

During the process of the chemical reaction, certain activators are usually required to influence the reaction. In studies on $NH_3$-N removal from wastewater, the addition of $Cl^-$ has been shown to significantly enhance the conversion of $NH_3$-N to $N_2$, indicating that chloride-containing species participate in the oxidation process [19–21]. Related studies have demonstrated that active chloride can be generated on the anode by applying a positive voltage. The electrochemically produced chloride participates in multiple steps of the ammonia oxidation process, substantially improving its efficiency [22–24]. These studies suggest that $Cl^-$ has the potential to increase the sensitivity of $NH_3$-N detection.

This study employs MEMS fabrication technology to develop an ultramicro UIAE chip for the detection of $NH_3$-N concentrations in neutral aqueous water. Unlike previous

studies, one comb of the UIAE functioned as both a modulation electrode and a sensor electrode, while the other was used as a counter electrode. The design of the ultramicro electrode structure was intended to achieve excellent redox performance and modulation ability. $Cl^-$, as a key activating agent, was added to the test solution at a concentration significantly higher than that of the target $NH_3$-N. A modulation process was utilized for the in situ activation of the electrochemical reaction of $NH_3$-N by modulating the local pH and active chloride in the vicinity of the electrode chip. Consequently, $NH_3$-N can be detected in neutral aqueous conditions with high sensitivity and stability. Furthermore, this detection allows the use of a single-channel electrochemical workstation rather than a dual-channel electrochemical workstation, thereby simplifying the detection system.

## 2. Materials and Methods

### *2.1. Instruments and Reagents*

The chemicals used in the experiments included acetone, ethanol, hydrochloric acid (HCl), sulfuric acid ($H_2SO_4$) (Beijing Chemical Factory, Beijing, China), phenolphthalein, KCl, $Na_2SO_4$, $(NH_4)_2SO_4$ (China National Pharmaceutical Group Chemical Reagent Co., Ltd., Shanghai, China), and NaOH (Shanghai Aladdin Biochemical Technology Co., Ltd., Shanghai, China). All reagents were of analytical grade.

The experimental equipment comprised a CHI660e electrochemical workstation, an Ag/AgCl reference electrode (CH Instruments, Shanghai, China), and a PHS-3C pH meter (Shanghai Leici Instruments Co., Ltd., Shanghai, China). All aqueous solutions used in this study were prepared using high-purity deionized water (Milli-Q system, Millipore, Darmstadt, Germany) with a resistivity of 18 MΩ·cm.

### *2.2. Design and Fabrication of the UIAE Chip*

The UIAE chip was composed of stripline working and counter electrodes arranged in an array on the surface of the insulating layer, as shown in Figure 1a. These electrodes are interleaved and individually connected by strip lead wires to form an approximate symmetry of a double-comb shape. The working electrode functioned as a modulation and sensor electrode. Previous studies have confirmed the excellent performance of UIAE in detecting $NH_3$-N in water, demonstrating that a smaller electrode width and smaller spacing-to-width ratio can enhance the microstructure characteristics, resulting in a higher sensitivity, and reduce the poisoning of Pt electrodes [25]. In this study, the electrodes were designed with a working electrode strip width of 5 μm, length of 2 mm, a spacing-to-width ratio of 5, and an array number of 80, providing an effective area of 0.8 $mm^2$. The entire electrode chip was 5 mm × 8 mm.

The UIAE chip fabrication process was investigated using the MEMS technique. The schematic of a certain fabrication procedure is shown in Figure 1b. Silicon wafers were selected as the substrate for the chip due to its moderate hardness, resistivity, excellent thermal stability, and chemical inertness. An insulating buried layer composed of silicon dioxide and nitride film was formed on the silicon surface before fabricating the metal electrode layer. Thermal oxidation and low-pressure chemical vapor deposition (LPCVD) techniques were used to fabricate the silicon dioxide and silicon nitride film, respectively. This layer isolates the silicon substrate from the metal electrodes, reducing leakage current and enhancing the electrical performance of the chip [26].

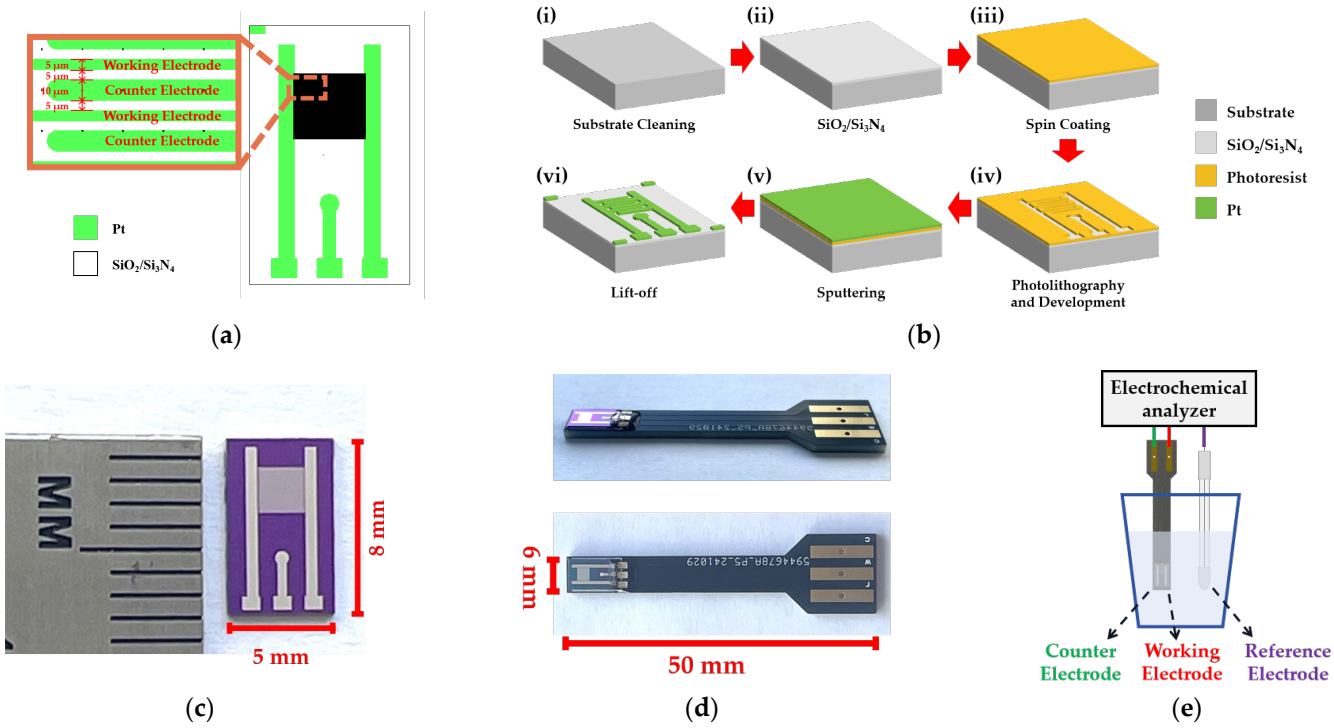


**Figure 1.** Ultramicro interdigitated array electrode (UIAE) chip: (**a**) design diagram, (**b**) fabrication process flowchart: (i) substrate cleaning, (ii) insulating buried layer fabrication, (iii) spin coating, (iv) photolithography and development, (v) sputtering and (vi) lift-off, (**c**) physical image, (**d**) encapsulated physical image, and (**e**) schematic of the three-electrode testing system.

Thin films of titanium (20 nm) and platinum (300 nm) were sputtered on the insulating layer to form the electrode layer. Platinum (Pt) is stable in electrochemical environments and provides active sites for various reactions. In addition, due to the weak adhesion between platinum and the underlying silicon nitride layer, a titanium film was selected as an adhesion layer to improve bonding. The working electrode and the counter electrode were formed through photolithography, sputtering, and the lifted-off process.

The fabricated silicon wafer was diced into individual chips (Figure 1c). After that, the individual electrode chip was electrically connected and packaged onto a PCB substrate. Insulating glue was used to encapsulate the bonding pads. The fabricated electrode chip is shown in Figure 1d.

### *2.3. Electrochemical Measurements*

The electrochemical detection of $NH_3$-N and related exploratory experiments were conducted using a three-electrode system (Figure 1e). The two-comb electrodes of the UIAE chip served as the working electrode and counter electrode, respectively. An Ag/AgCl (3 M KCl) electrode was used as the reference electrode. An external potential was applied between the working electrode and the reference electrode using an electrochemical workstation, inducing electrochemical reactions on the surface of the working electrode. The current flowed through the counter electrode, and the concentration of the analyte was calculated by detecting the response current. The reference electrode, which does not pass current, provided a stable reference potential.

All electrochemical experiments were performed on a CHI660e electrochemical workstation (CH Instruments Inc., Bee Cave, TX, USA). Before testing, the three-electrode system was immersed in 0.05 M $H_2SO_4$, and cyclic voltammetry (CV) scanning was conducted over the range of −0.25 to 1.2 V for several cycles until the response curve stabilized. Differential pulse voltammetry (DPV) was employed for $NH_3$-N electrochemical detec-

tion. Before the implementation of DPV detection, a modulation potential of 1.2 V was applied for 20 s for the in situ regulation of the local pH and active chloride near the UIAE chip. The optimization of the modulation parameters is detailed in Section 3.2. The DPV measurements were conducted within a range of −0.6 V to 0 V, with a pulse amplitude of 50 mV, a step of 5 mV, a pulse width of 20 ms, and a pulse period of 50 ms. The duration of the DPV detection process was 6 s. The neutral electrolyte solution used for $NH_3$-N electrochemical detection was 0.2 M KCl. For the purpose of comparison, a strong alkaline solution containing 0.2 M KCl and 1 M NaOH was also utilized, as is generally required for the detection of $NH_3$-N, without using the in situ electrochemical modulation process. All test solutions were degassed with excess argon gas to remove dissolved oxygen and other interfering gases prior to experimentation.

## 3. Results and Discussion

### *3.1. Detection of $NH_3$-N with UIAEs in an Alkaline Environment*

For comparison, the UIAE chip was first used for the detection of $NH_3$-N in a strongly alkaline environment. DPV was employed for quantitative detection by adding $NH_3$-N to a 0.2 M KCl and 1 M NaOH solution. As shown in Figure 2a, current response peaks appeared in the potential ranges from −0.5 V to −0.3 V and −0.25 V to −0.1 V. Among these, the oxidation peak in the range of −0.5 V to −0.3 V gradually increased as the $NH_3$-N concentration rose from 0.15 to 2.0 mg/L (as N). Figure 2b illustrates the relationship between the peak current in the range of −0.5 V to −0.3 V and $NH_3$-N concentration, with segmented linear relationships in the ranges of 0.15 to 1.0 mg/L and 1.0 to 2.0 mg/L, and the sensitivities were 1.5499 μA·L·mg$^{-1}$ and 0.4904 μA·L·mg$^{-1}$. The current exhibited a trend toward saturation as the concentration increased.

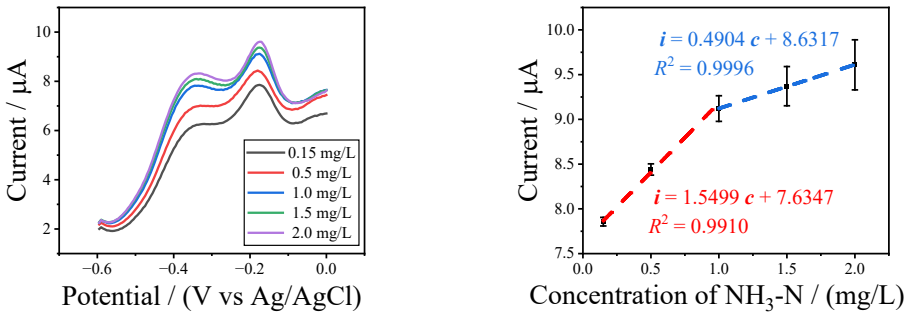


**Figure 2.** (**a**) DPV response curve with certain ammonia nitrogen ($NH_3$-N) concentration from 0.15 to 2.0 mg/L and (**b**) corresponding calibration curve of peak current vs. concentration of $NH_3$-N in an alkaline environment (pH = 14).

The experimental results confirm that the UIAE chip, combined with the DPV method, can effectively trigger the oxidation of $NH_3$-N. In a strongly alkaline environment, chloride exists in the form of hypochlorite ($ClO^-$). $ClO^-$ has strong chemical reactivity and can act as an oxidizing agent to facilitate the electrochemical oxidation of ammonia under electrocatalytic conditions. When testing with the UIAE electrode, the oxidation peak shifts from approximately −0.2 V (as shown in other literature [25]) to around −0.4 V. This indicates that an increase in chloride concentration in the solution not only affects the sensitivity of the current response to the $NH_3$-N concentration but also alters the reaction mechanism. Based on the experimental results, the oxidation peak at approximately −0.4 V is inferred to be associated with the chloride-assisted electrocatalytic oxidation of $NH_3$-N. In chloride-containing environments, the oxidation peak at −0.2 V remains, suggesting that $NH_3$-N oxidation facilitated by an alkaline environment still occurs. However, its

correlation with concentration is influenced by competition with the chloride-assisted oxidation at −0.4 V.

### *3.2. In Situ Modulation Performance of UIAEs in a Neutral Environment*

The in situ modulation capability of the electrode was investigated to evaluate its effectiveness in creating localized pH changes near the electrode surface. Experiments were conducted using a 0.2 M KCl solution containing phenolphthalein (pH = 7.5). Phenolphthalein, with a color change range of 8.2–10, transitions from colorless to purple as the pH increases and as the solution becomes more alkaline. By applying an electric potential, the primary reaction in the solution is electrolysis of the KCl solution. In this case, the electrochemical reaction at the cathode mainly generates $OH^-$, while the anode produces $Cl_2$. The proximity effect and the rapid mass transfer characteristics of UIAE result in a significant overlap of the diffusion zones of the interdigitated electrode pairs. Therefore, the $OH^-$ produced at the cathode makes the solution alkaline in the vicinity of both the cathode and the anode. The product $Cl_2$ from the anode reaction reacts with $OH^-$ to form $ClO^-$ [21], which can further promote the oxidation of $NH_3$-N. In order to optimize the applied potential, 0.9 V, 1.2 V, 1.5 V, and 1.8 V were selected for testing. As shown in Figure 3, color changes in the solution were recorded at 10 s, 20 s, and 30 s during the modulation application and 10 s after the modulation ended.

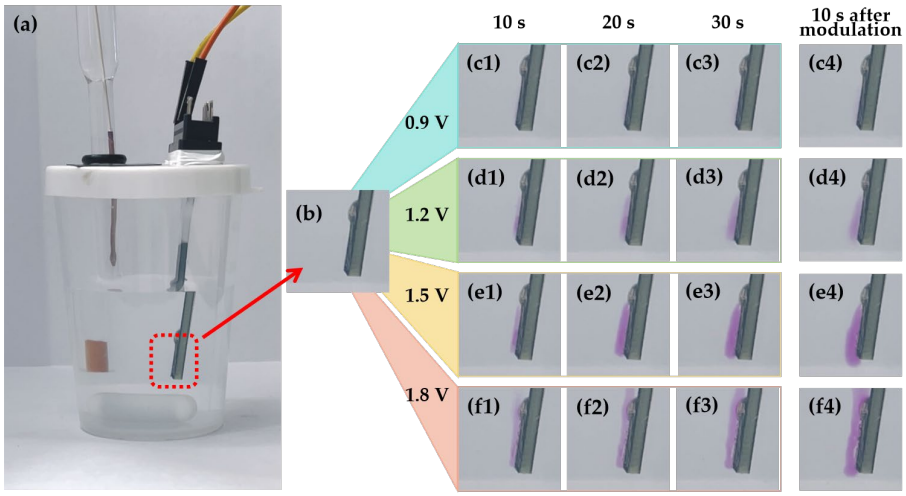


**Figure 3.** Photos of the UIAE chip in situ pH modulation capability testing: (**a**) the testing setup,linebreak (**b**) the area near the UIAE chip without applying potential, and when applying potentials of (**c1–c4**) 0.9 V, (**d1–d4**) 1.2 V, (**e1–e4**) 1.5 V, and (**f1–f4**) 1.8 V for 30 s, showing the results at 10 s, 20 s, 30 s, and 10 s after the modulation process.

When a 0.9 V potential was applied, no significant color change was observed near the UIAE chip (Figure 3(c1–c4)). However, when potentials of 1.2 V, 1.5 V, and 1.8 V were applied, a color change occurred in the solution near the UIAE chip (Figure 3(d1,e1,f1)). The intensity of the color increased with the duration of the applied potential (Figure 3(d2,d3,e2,e3,f2,f3)), indicating that the pH near the UIAE chip shifted from neutral to alkaline, with the duration of the potential application affecting the strength of the alkalinity. However, when potentials of 1.5 V and 1.8 V were applied, bubbles were generated on the chip surface (Figure 3(e1–e4,f1–f4)). Ten seconds after the modulation process ended, the colored area expanded slightly, but the intensity of the color change remained largely unchanged (Figure 3(d4,e4,f4)). These results indicate that the in situ modulation effect has the ability to persist for a period of time after the termination of the modulation potential, and the duration is sufficient for the conduction of a subsequent DPV measurement of 6 s.

The experimental results demonstrate that applying a constant potential of 1.2 V or higher to the working electrode of the UIAE chip can achieve localized in situ modulation. The modulation effect remained stable for up to 10 s after the potential application, indicating that a single electrode can be used in a time-division multiplexing manner for post-modulation detection experiments. However, increasing the potential to 1.5 V or higher caused bubble formation around the electrode, reducing the contact area between the electrode surface and the reaction solution and interfering with subsequent experiments.

The feasibility of $NH_3$-N detection using this UIAE chip in a near-neutral environment with in situ electrochemical modulation was verified. Based on the in situ pH modulation experimental results, the modulation potential of 1.2 V with a treatment duration of 20 s was selected. After modulation, the electrochemical response of the test solution was measured using the DPV method. Tests were conducted in a neutral environment (0.2 M KCl) with and without the in situ modulation step before and after the addition of $NH_3$-N. As shown in Figure 4a, in the absence of in situ modulation, no significant current peak or current change response to $NH_3$-N was observed in the neutral environment. With in situ modulation, a distinct oxidation peak appeared in a range from −0.5 V to −0.3 V. The peak current increased from 3.96 μA to 8.32 μA with the addition of 1 mg/L $NH_3$-N. These results demonstrate that in situ modulation enables the UIAE chip to detect $NH_3$-N in a neutral environment using KCl as the base solution.

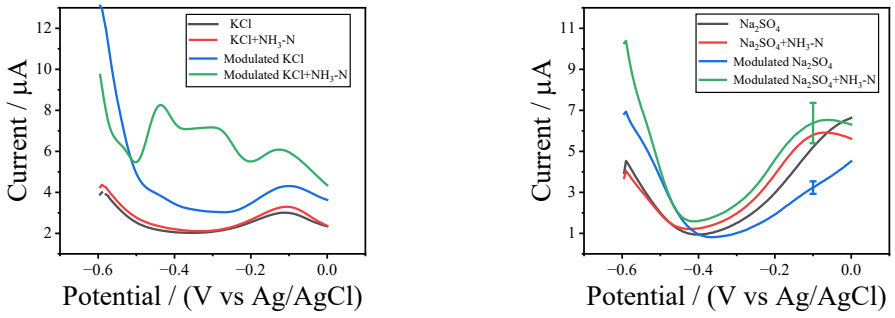


(**a**) (**b**)

**Figure 4.** The effect of the in situ modulation process on the DPV response characteristics of $NH_3$-N in neutral environments (pH = 7.5) with different electrolytes: (**a**) KCl and (**b**) $Na_2SO_4$.

To investigate the effect of $Cl^-$ on in situ modulation and $NH_3$-N detection, similar experiments were conducted on a test solution containing 0.2 M $Na_2SO_4$ (pH = 7.5). The results are shown in Figure 4b. Under these conditions, no oxidation peak or response current appeared around −0.4 V. Additionally, an oxidation peak emerged at −0.1 V after in situ modulation, but it exhibited significant variability across multiple tests.

The results demonstrate that excess $Cl^-$ enhances $NH_3$-N detection via modulation. During in situ modulation, $OH^-$ and $ClO^-$ generated from electrolyte electrolysis promote $NH_3$-N oxidation, enabling electrochemical detection in neutral environments. At this point, the peak-to-peak position of the DPV response using KCl as the base solution with modulation (shown in Figure 4a) is close to the DPV test peak position under alkaline chlorinated conditions (shown in Figure 2a). This further supports the conclusion that the in situ modulation method provides a localized $NH_3$-N detection environment near the electrode.

When the electrolyte is switched to $Na_2SO_4$, the low chloride content reduces the production of chlorinated species during in situ modulation, causing significant deviations in the DPV response curve in repeated tests. However, the modulated system still produces a response peak for $NH_3$-N, with its position aligning more closely with the results under non-chlorinated conditions. Modulation occurs via water electrolysis, generating $OH^-$ near the electrode, which aids $NH_3$-N oxidation. Additionally, trace chloride from the

Ag/AgCl reference electrode can enter the solution, leading to uncontrollable fluctuations in the chloride species' concentration and causing variability in the promoting effect of $ClO^-$ on $NH_3$-N oxidation during repeated tests.

The influence of the modulation duration on the DPV response current of $NH_3$-N was also investigated. A modulation potential of 1.2 V was chosen. The response currents of the UIAE chip in a 1 mg/L $NH_3$-N solution were detected using different modulation durations. The DPV detecting curves and the oxidation peak currents are shown in Figure 5. As the modulation duration increased, the response current increased. However, when the modulation duration exceeded 15 s, the response current no longer increased significantly. The experimental results indicate that for modulation durations shorter than 15 s, the increase in applied potential time led to an enhancement in alkalinity and in the concentration of active chloride in the solution in the vicinity of the UIAE chip. This, in turn, induced a catalytic effect and promoted the electrochemical oxidation of $NH_3$-N. When the modulation duration exceeded 15 s, the promoting effect reached its upper limit, and the response intensity to $NH_3$-N no longer improved. In consideration of the effect of this catalytic limit on the linear detection range, and with the aim of minimizing the detection time, a modulation duration of 20 s was selected for the subsequent experiments.

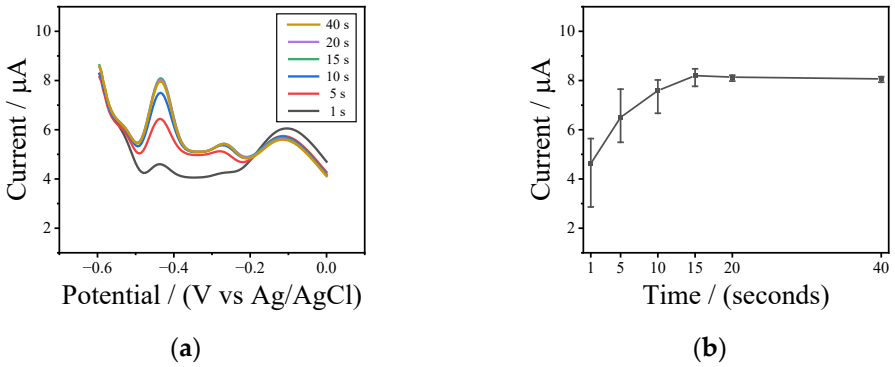


**Figure 5.** Optimization of the in situ modulation time in neutral environments (pH = 7.5): (**a**) DPV response curves and (**b**) peak current results and error bars for different modulation durations.

### *3.3. Detection of $NH_3$-N with UIAEs in a Neutral Environment*

Based on the experiments conducted earlier, the $NH_3$-N detection based on the in situ modulation proposed in this paper (as shown in Figure 6) can be described as follows: In the in situ modulation step, the neutral KCl aqueous environment near the electrode surface undergoes electrolysis, generating $Cl_2$ and $OH^-$, which further forms $ClO^-$, creating an alkaline environment near the electrode. In the DPV testing step, $NH_3$-N behaves as $NH_3$ under alkaline conditions, which undergoes electrocatalytic oxidation between the electrodes with the help of $ClO^-$.

The response current of the UIAE chip to different concentrations of $NH_3$-N in a neutral environment was investigated using the in situ modulation technique. $NH_3$-N was added to 0.2 M KCl for quantitative detection. A constant potential of 1.2 V was applied for a duration of 20 s before DPV measurement. As shown in Figure 7a, a concentration-dependent current peak appeared in the potential range of −0.5 V to −0.3 V, and the peak current gradually increased as the $NH_3$-N concentration rose from 0.15 to 2.0 mg/L (as N). Figure 7b illustrates the relationship between the peak current and $NH_3$-N concentration. Within the concentration range of 0.15–2.0 mg/L, the peak current exhibited a linear relationship with the $NH_3$-N concentration, described by the linear regression equation $i$ (μA) = 3.7936 $c$ (mg/L) + 4.0736 ($R^2$ = 0.9848). The sensitivity increased to 3.7936 μA·L·$mg^{-1}$, which was 2.45 times that in strong alkaline conditions without modulation. This demonstrates that

the in situ modulation technique significantly enhances the detection of $NH_3$-N in neutral aqueous environments.

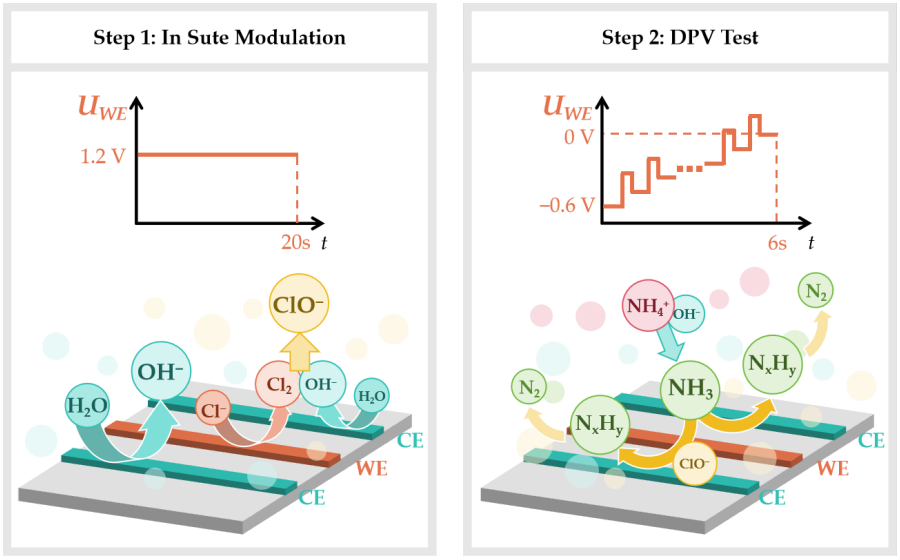


**Figure 6.** Schematic of $NH_3$-N detection based on in situ modulation in neutral environments using the UIAE chip.

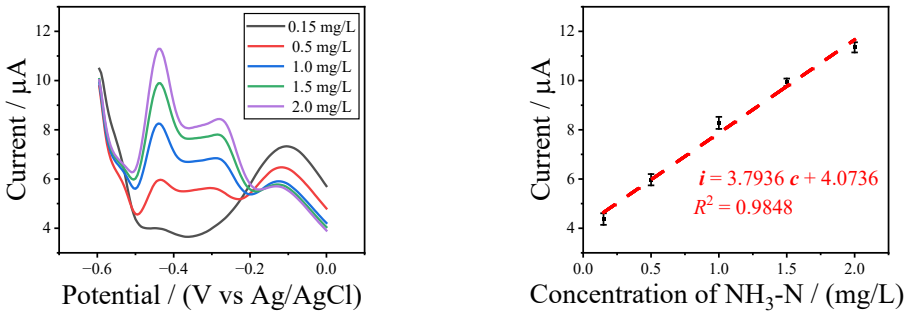


**Figure 7.** (**a**) DPV response curve with certain $NH_3$-N concentrations from 0.15 to 2.0 mg/L in neutral environments (pH = 7.5), and the (**b**) calibration curve of peak current vs. concentration of $NH_3$-N.

The limit of detection (LOD) was determined by repeating the UIAE in situ modulation-based $NH_3$-N detection process seven times on blank solutions and recording the response current values. Based on the three times signal-to-noise ratio calculation formula, the calculated LOD was 0.0481 mg/L.

### *3.4. Anti-Interference Ability and Selectivity*

In the $NH_3$-N test solution containing 1 mg/L, 10 times the concentration (10 mg/L) of $Na^+$, $CO_3^{2-}$, $SO_3^{2-}$, $HCO_3^-$, and $NO_3^-$ was added, and the solutions with and without interfering ions were tested. The response current for the 1 mg/L $NH_3$-N solution without interfering ions was taken as 100%, and the response current for the solution with interfering ions was recorded as a percentage relative to the response current without interfering ions. The anti-interference test results are shown in Figure 8a. According to the test results, the deviation in the response current caused by the interfering ions tested was all less than 10%. Among them, the deviation caused by $NO_3^-$ was the largest, at 8.88%. The experimental results indicate that these interfering ions have a minimal effect on the response results of this detection method, demonstrating the method's good anti-interference performance.

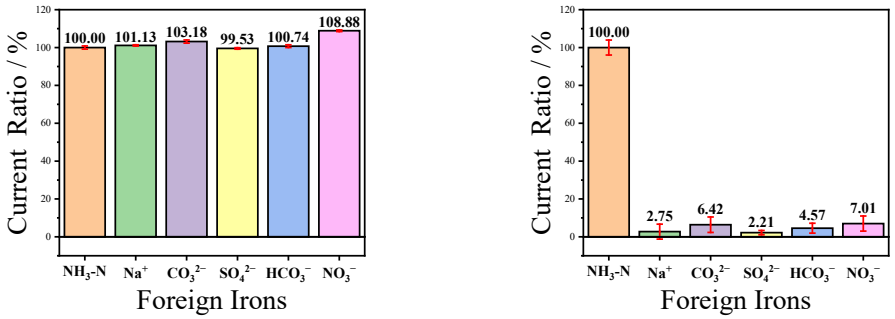


**Figure 8.** (**a**) Interference test results and (**b**) selectivity test results at a $NH_3$-N concentration of 1 mg/L in the presence of interfering ions at a concentration of 10 mg/L.

In a solution without $NH_3$-N, 10 times the concentration (10 mg/L) of $Na^+$, $CO_3^{2-}$, $SO_3^{2-}$, $HCO_3^-$, and $NO_3^-$ was added, and the test solution before and after adding the interfering ions was tested repeatedly. The change in the response current was recorded and compared with the response current of the 1 mg/L $NH_3$-N solution, and the results are shown in Figure 8b. Among the interfering ions tested, the $NO_3^-$ with 10 times the concentration caused the largest change in response current at 7.01%. The response current caused by $CO_3^{2-}$ was the second largest, at 6.42%. The response currents caused by the other interfering ions were all less than 5%, indicating that the method has good selectivity.

### *3.5. Repeatability and Stability*

The repeatability and stability of the UIAE chip for $NH_3$-N detection were evaluated using the in situ modulation method. Five consecutive repeated tests were performed on a 1 mg/L $NH_3$-N test solution. The response currents and oxidation peak results are shown in Figure 9a, with a relative standard deviation (RSD) of 1.98%. Additionally, repeated tests were conducted over five days on $NH_3$-N test solutions with concentrations of 0.15 mg/L, 1 mg/L, and 2 mg/L. The peak response current results are shown in Figure 9b, with RSD values of 2.77%, 2.82%, and 1.78%.

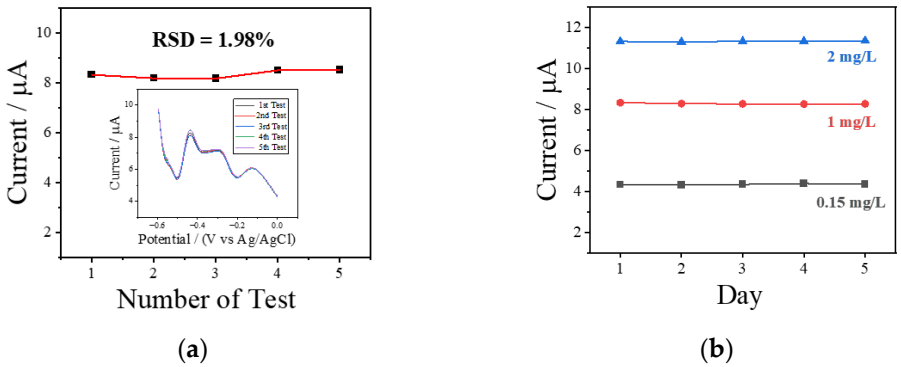


**Figure 9.** (**a**) DPV curves and peak currents of 5 repeated tests on solutions containing 1 mg/L $NH_3$-N and (**b**) peak currents of 5 days of stability tests on solutions containing 0.15, 1, and 2 mg/L $NH_3$-N.

Table 1 shows a comparison of the performance of the UIAE chip with other reported $NH_3$-N electrochemical sensors. To enable easy comparison, the concentration units have been converted to molar units. The sensitivity expressed in current density units is 0.0664 μA $\mu M^{-1}$ $mm^{-2}$ when normalized to the effective electrode area. Previous studies in the literature most commonly report the detection of $NH_3$-N in strongly alkaline solutions, while some employed acidic solutions. In contrast, this work utilizes an in

situ modulation approach, enabling detection in near-neutral environments. Additionally, this sensor chip achieves high sensitivity and excellent stability without the need for nanomaterial modification.

**Table 1.** Performance comparison of different $NH_3$-N electrochemical sensors.

| Electrode Type | Substrate Solution | Method | Detection Range (μM) | Sensitivity (μA μM$^{-1}$ mm$^{-2}$) | Detection Limit (μM) | RSD (%) | Ref |
|---|---|---|---|---|---|---|---|
| AuNPs/CC@G | 0.1 M KOH | CV | $1 \times 10^{-3}$–10,000 | 6.4477 | $9.84 \times 10^{-4}$ | 1.11 | [5] |
| PtCu/CC | 1 M KOH | DPV | 0.5–40<br>40–500 | 0.0940<br>0.0078 | $8.6 \times 10^{-3}$ | 0.60 | [27] |
| PtNi/CC | 1 M KOH | DPV | 0.5–150<br>150–500 | 0.0783<br>0.0095 | $2.4 \times 10^{-2}$ | 1.85 | [28] |
| PtZn NFs/CC | 1 M KOH | DPV | 1–100<br>100–400 | 0.4300<br>0.1178 | $2.78 \times 10^{-2}$ | 4.68 | [7] |
| Pt NPs-Pt Wire | 0.1 M $Na_2SO_4$ (pH = 3) | LSV | 45–64,000 | 0.0662 | 45 | / | [29] |
| Pt UIAE | 0.2 M $Na_2HPO_4$ (pH = 10) | DPV | 10.7–142.9 | 0.0098 | 1.77 | 2.90 | [25] |
| Pt UIAE | 1 M NaOH | DPV | 10.7–71.45 | 0.0273 | / | / | This work |
| Pt UIAE | 0.2 M KCl (pH = 7.5) | DPV with modulation | 10.7–142.9 | 0.0664 | 3.44 | 1.98 | This work |

AuNPs/CC@G: carbon cloth self-contained electrode modified with gold nanoparticles wrapped with graphene nanosheets; PtCu/CC: carbon cloth self-supporting electrode modified with PtCu alloy nanomaterials; PtNi/CC: carbon cloth self-supporting electrode modified with PtNi alloy nanomaterials; PtZn NFs-/CC: carbon cloth self-supporting electrode modified with PtZn alloy nanomaterials; Pt NPs-Pt Wire: drawing Pt wire modified by Pt nanoparticles.

## 4. Conclusions

An in situ modulation and determination method based on a UIAE chip was developed for the detection of $NH_3$-N in neutral aqueous solutions. Utilizing the rapid mass transfer characteristics of the UIAE chip, the local pH value and the active chloride concentration near the UIAE chip were enhanced by applying a certain potential before $NH_3$-N electrochemical oxidation. This work demonstrated the feasibility of electrochemical $NH_3$-N detection under neutral conditions without the need for strong alkaline additives, significantly reducing secondary contamination of water samples and the corrosion of the sensor system. With these features, this determination method has the potential for on-site $NH_3$-N monitoring.

**Author Contributions:** Conceptualization, C.B., Y.L. (Yuqi Liu) and Y.L. (Yang Li); methodology, C.B., Y.L. (Yang Li) and Y.L. (Yuqi Liu); validation, Y.L. (Yuqi Liu), N.Q. and Z.Z.; data curation, Y.L. (Yuqi Liu), N.Q. and Z.Z.; writing—original draft preparation, Y.L. (Yuqi Liu); writing—review and editing, C.B. and Y.L. (Yang Li); visualization, Y.L. (Yuqi Liu); supervision, C.B. and Y.L. (Yang Li); project administration, C.B.; funding acquisition, C.B. All authors have read and agreed to the published version of the manuscript.

**Funding:** This research is supported by the National Natural Science Foundation of China (No. 62271472).

**Institutional Review Board Statement:** Not applicable.

**Informed Consent Statement:** Not applicable.

**Data Availability Statement:** The data that support the findings of this study are available from the corresponding author upon reasonable request.

**Conflicts of Interest:** The authors declare no conflicts of interest.

## References

1. Wen, Y.; Mao, Y.; Kang, Z.; Luo, Q. Application of an Ammonium Ion-Selective Electrode for the Real-Time Measurement of Ammonia Nitrogen Based on Ph and Temperature Compensation. *Measurement* **2019**, *137*, 98–101. [CrossRef]
2. Gerischer, H.; Mauerer, A. Untersuchungen Zur Anodischen Oxidation Von Ammoniak an Platin-Elektroden. *J. Electroanal. Chem.* **1970**, *25*, 421–433. [CrossRef]
3. Vidal-Iglesias, F.J.; Solla-Gullón, J.; Rodríguez, P.; Herrero, E.; Montiel, V.; Feliu, J.M.; Aldaz, A. Shape-Dependent Electrocatalysis: Ammonia Oxidation on Platinum Nanoparticles with Preferential (100) Surfaces. *Electrochem. Commun.* **2004**, *6*, 1080–1084. [CrossRef]
4. Elnabawy, A.O.; Herron, J.A.; Karraker, S.; Mavrikakis, M. Structure Sensitivity of Ammonia Electro-Oxidation on Transition Metal Surfaces: A First-Principles Study. *J. Catal.* **2021**, *397*, 137–147. [CrossRef]
5. Qin, R.; Zhang, Y.; Xu, H.; Nie, P. Gold Nanoparticle-Modified Electrodes for Electrochemical Sensing of Ammonia Nitrogen in Water. *ACS Appl. Nano Mater.* **2023**, *7*, 577–593. [CrossRef]
6. Zhou, G.; Wang, G.; Zhao, X.; He, D.; Zhao, C.; Suo, H. Electrochemical Detection of Ammonia in Water Using Nicu Carbonate Hydroxide-Modified Carbon Cloth Electrodes: A Simple Sensing Method. *Sensors* **2024**, *24*, 4824. [CrossRef]
7. Wang, G.; Zhou, G.; Zhang, Q.; He, D.; Zhao, C.; Suo, H. Sensitive Electrochemical Detection of Ammonia Nitrogen Via a Platinum-Zinc Alloy Nanoflower-Modified Carbon Cloth Electrode. *Sensor* **2024**, *24*, 915. [CrossRef]
8. Blume, S.O.P.; Ben-Mrad, R.; Sullivan, P.E. Modelling the Capacitance of Multi-Layer Conductor-Facing Interdigitated Electrode Structures. *Sens. Actuators B Chem.* **2015**, *213*, 423–433. [CrossRef]
9. Yagati, A.K.; Park, J.; Cho, S. Reduced Graphene Oxide Modified the Interdigitated Chain Electrode for an Insulin Sensor. *Sensors* **2016**, *16*, 109. [CrossRef]
10. Liu, N.; Gao, Y. Recent Progress in Micro-Supercapacitors with in-Plane Interdigital Electrode Architecture. *Small* **2017**, *13*, 1701989. [CrossRef]
11. Kosri, E.; Ibrahim, F.; Thiha, A.; Madou, M. Micro and Nano Interdigitated Electrode Array (Idea)-Based Mems/Nems as Electrochemical Transducers: A Review. *Nanomaterials* **2022**, *12*, 4171. [CrossRef] [PubMed]
12. Pastre, A.; Boé, A.; Rolland, N.; Bernard, R. All-Solid-State Interdigitated Micro-Supercapacitors Based on Porous Gold Electrodes. *Sensors* **2023**, *23*, 619. [CrossRef] [PubMed]
13. Zhao, S.; Tong, J.; Li, Y.; Sun, J.; Bian, C.; Xia, S. Palladium-Gold Modified Ultramicro Interdigital Array Electrode Chip for Nitrate Detection in Neutral Water. *Micromachines* **2019**, *10*, 223. [CrossRef] [PubMed]
14. Patella, B.; O'Sullivan, B.; Daly, R.; Lovera, P.; Inguanta, R.; O'Riordan, A. *Simultaneous Detection of Copper, Lead and Mercury in River Water with in-Situ Ph Control Using Electrochemical Stripping Techniques*, Tyndall National Institute: Cork, Ireland, 2020; unpublished work.
15. Seymour, I.; O'Sullivan, B.; Lovera, P.; Rohan, J.F.; O'Riordan, A. Electrochemical Detection of Free-Chlorine in Water Samples Facilitated by in-Situ Ph Control Using Interdigitated Microelectrodes. *Sens. Actuators B Chem.* **2020**, *325*, 128774. [CrossRef]
16. O'Sullivan, B.; Patella, B.; Daly, R.; Seymour, I.; Robinson, C.; Lovera, P.; Rohan, J.; Inguanta, R.; O'Riordan, A. A Simulation and Experimental Study of Electrochemical Ph Control at Gold Interdigitated Electrode Arrays. *Electrochim. Acta* **2021**, *395*, 139113. [CrossRef]
17. Seymour, I.; O'Sullivan, B.; Lovera, P.; Rohan, J.F.; O'Riordan, A. Elimination of Oxygen Interference in the Electrochemical Detection of Monochloramine, Using in Situ Ph Control at Interdigitated Electrodes. *ACS Sens.* **2021**, *6*, 1030–1038. [CrossRef]
18. Wasiewska, L.A.; Seymour, I.; Patella, B.; Inguanta, R.; Burgess, C.M.; Duffy, G.; O'Riordan, A. Reagent Free Electrochemical-Based Detection of Silver Ions at Interdigitated Microelectrodes Using in-Situ Ph Control. *Sens. Actuators B Chem.* **2021**, *333*, 129531. [CrossRef]
19. Li, L.; Liu, Y. Ammonia Removal in Electrochemical Oxidation: Mechanism and Pseudo-Kinetics. *J. Hazard. Mater.* **2009**, *161*, 1010–1016. [CrossRef]
20. Zhang, C.; He, D.; Ma, J.; Waite, T.D. Active Chlorine Mediated Ammonia Oxidation Revisited: Reaction Mechanism, Kinetic Modelling and Implications. *Water Res.* **2018**, *145*, 220–230. [CrossRef]
21. Li, Q.; Liu, G.H.; Du, H.; Xian, G.; Qi, L.; Wang, H. Synergistic Mechanisms between Chlorine-Mediated Electrochemical Advanced Oxidation and Ultraviolet Light for Ammonia Removal. *J. Environ. Manag.* **2024**, *352*, 120057. [CrossRef]
22. Zhang, Y.; Li, J.; Bai, J.; Li, L.; Chen, S.; Zhou, T.; Wang, J.; Xia, L.; Xu, Q.; Zhou, B. Extremely Efficient Decomposition of Ammonia N to N2 Using Clo from Reactions of Ho and Hocl Generated in Situ on a Novel Bifacial Photoelectroanode. *Environ. Sci. Technol.* **2019**, *53*, 6945–6953. [CrossRef] [PubMed]

23. Huang, X.; Zhang, Y.; Bai, J.; Li, J.; Li, L.; Zhou, T.; Chen, S.; Wang, J.; Rahim, M.; Guan, X.; et al. Efficient Degradation of N-Containing Organic Wastewater Via Chlorine Oxide Radical Generated by a Photoelectrochemical System. *Chem. Eng. J.* **2020**, *392*, 123695. [CrossRef]
24. Zhang, Y.; Tang, W.; Bai, J.; Li, J.; Wang, J.; Zhou, T.; Guan, X.; Zhou, B. Highly Efficient Removal of Total Nitrogen and Dissolved Organic Compound in Waste Reverse Osmosis Concentrate Mediated by Chlorine Radical on 3d Co3o4 Nanowires Anode. *J. Hazard. Mater.* **2022**, *424*, 127662. [CrossRef] [PubMed]
25. Zhao, H.; Li, Y.; Cong, A.; Tong, J.; Bian, C. Ultramicro Interdigitated Array Electrode Chip with Optimized Construction for Detection of Ammonia Nitrogen in Water. *Micromachines* **2023**, *14*, 629. [CrossRef]
26. Kaloyeros, A.E.; Pan, Y.; Goff, J.; Arkles, B. Review—Silicon Nitride and Silicon Nitride-Rich Thin Film Technologies: State-of-the-Art Processing Technologies, Properties, and Applications. *ECS J. Solid State Sci. Technol.* **2020**, *9*, 063006. [CrossRef]
27. Wang, G.; Gao, J.; Sun, B.; He, D.; Zhao, C.; Suo, H. Enhanced Ammonia Sensitivity Electrochemical Sensors Based on Ptcu Alloy Nanoparticles in-Situ Synthesized on Carbon Cloth Electrode. *J. Electroanal. Chem.* **2022**, *922*, 116721. [CrossRef]
28. Wang, G.; Ma, G.; Gao, J.; He, D.; Zhao, C.; Suo, H. Enhanced Sensitivity of Electrochemical Sensors for Ammonia-Nitrogen Via in-Situ Synthesis Ptni Nanoleaves on Carbon Cloth. *Sensors* **2024**, *24*, 387. [CrossRef]
29. Ning, Y.-F.; Yan, P.; Chen, Y.-P.; Guo, J.-S.; Shen, Y.; Fang, F.; Tang, Y.; Gao, X. Development of a Pt Modified Microelectrode Aimed for the Monitoring of Ammonium in Solution. *Int. J. Environ. Anal. Chem.* **2017**, *97*, 85–98. [CrossRef]


**Disclaimer/Publisher's Note:** The statements, opinions and data contained in all publications are solely those of the individual author(s) and contributor(s) and not of MDPI and/or the editor(s). MDPI and/or the editor(s) disclaim responsibility for any injury to people or property resulting from any ideas, methods, instructions or products referred to in the content.